

Probabilistic Semantic Mapping for Urban Autonomous Driving Applications

*David Paz¹, *Hengyuan Zhang¹, *Qinru Li¹, *Hao Xiang¹, Henrik Christensen¹

Abstract—Recent advancement in statistical learning and computational ability has enabled autonomous vehicle technology to develop at a much faster rate and become widely adopted. While many of the architectures previously introduced are capable of operating under highly dynamic environments, many of these are constrained to smaller-scale deployments and require constant maintenance due to the associated scalability cost with high-definition (HD) maps. HD maps provide critical information for self-driving cars to drive safely. However, traditional approaches for creating HD maps involves tedious manual labeling. As an attempt to tackle this problem, we fuse 2D image semantic segmentation with pre-built point cloud maps collected from a relatively inexpensive 16 channel LiDAR sensor to construct a local probabilistic semantic map in bird’s eye view that encodes static landmarks such as roads, sidewalks, crosswalks, and lanes in the driving environment. Experiments from data collected in an urban environment show that this model can be extended for automatically incorporating road features into HD maps with potential future work directions.

I. INTRODUCTION

High-definition (HD) maps provide useful information for autonomous vehicles to understand the static parts of the scene. Due to the nature of the information encoded in HD maps—such as centimeter-level definitions for road networks, traffic signs, crosswalks, stop signs, traffic lights and even speed limits—many of these maps become outdated during construction or road network changes. Given these fast-changing environments, manually annotated HD maps become obsolete and may cause vehicles to perform inadequate reference path tracking actions leading to unsafe scenarios. In the process of HD map generation, extracting semantics and attributes from data takes the most amount of the work [1]. A model that automates this process could improve HD map generation, reducing labor cost, and increase driving safety.

Retrieval of centimeter-level semantic labels of the scene is a non-trivial task. Prior work such as [2], [3] adopted Conditional Random Fields (CRF) to assign semantic labels. The advancement of deep learning provides promising results in terms of retrieving semantic information from images. State of the art semantic segmentation algorithms such as [4], [5], [6] generate pixel level semantic label with greater accuracy. Researchers have also explored methods to create semantic mapping in the environment. Examples are given in [7], [8], [9]. Multi-sensor fusion is used to improve the robustness of the algorithm. However, these approaches either use aerial imagery to extract road information or do

not explicitly map the lane and crosswalk information, which are required for HD maps. A detailed semantic map for urban autonomous vehicle applications is still of interest to explore.

Our work is focused on leveraging dense point maps built from a 16 channel LiDAR and state of the art semantically labeled images from deep neural networks, trained only on a publicly available dataset, to automatically generate dense probabilistic semantic maps in urban driving environments that provide robust labels for roads, lanes, crosswalks, and sidewalks. The comparison with a real HD map that has been tested in our autonomous vehicle for campus mail delivery tasks shows that the proposed model can identify semantic features in the road and localize them accurately in 3D space.

II. RELATED WORK

Semantic Segmentation: Semantic segmentation is the task of assigning each observed data point (e.g. pixel or voxel) to a class label that contains semantic meanings. Research in this field has made tremendous progress as deep learning emerges and large scale datasets like CityScapes [10], CamVid [11], Mapillary[12], become available. As HD maps require centimeter-level labeling accuracy for each object, building such maps can significantly benefit from the pixel level information provided by semantic segmentation algorithms.

In 2D semantic segmentation, predominant works [4], [5], [13] leverage pyramid like encoder-decoder architecture to capture both global and local information in the images. Trained on the large scale datasets aforementioned, these network architectures can easily detect objects on the road even when these objects only have textural difference like colors. In 3D semantic segmentation, work has also been done by projecting 3D LiDAR point clouds into 2D image space and then feeding them to a classic CNN network to classify each point[14], [15], [16]. While the results of these works seem promising, due to the nature of LiDAR sensors, these methods cannot distinguish objects with texture difference such as colors. Researchers have also proposed an alternative approach of segmentation on voxelized point clouds [17]. However, such 3D convolution is computationally expensive and usually requires dense raw point cloud measurements (i.e 32/64 channel LiDARs), making it troublesome to operate in real time.

Semantic Mapping: Semantic mapping, has a rich meaning in various literature [18]. We adopted the definition closest to our context, defined in [19], which is the process of building maps that represent not only an occupancy metric but also other properties of the environment. Specifically, in

*These members contributed equally to this publication.

¹Contextual Robotics Institute, University of California, San Diego, 9500 Gilman Dr, La Jolla, CA 92093

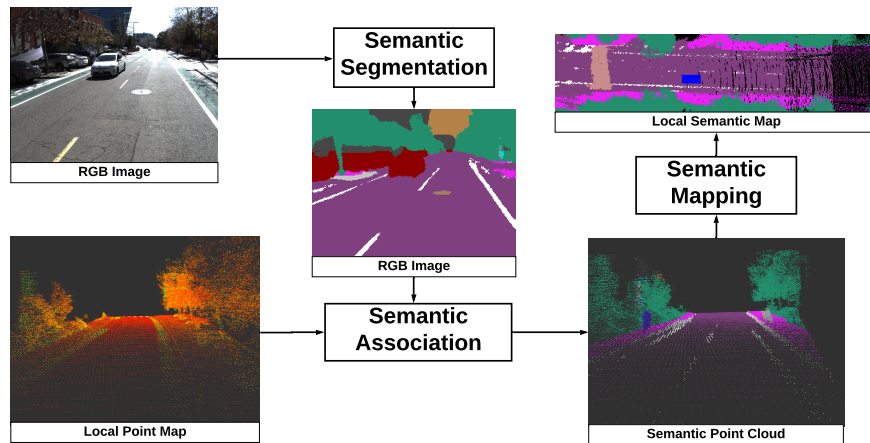


Fig. 1. Our pipeline for generating probabilistic semantic maps for road feature extraction and HD mapping applications.

the driving scenario, we focus on driveable surfaces and road marks.

Sunando et. al. [3] proposed a CRF based method in dense semantic mapping. They use associative hierarchical CRF for semantic segmentation and pairwise CRF for mapping. The pairwise potential minimization enforces the output smoothness. In [20], a stereo pair is used to provide robust depth estimation, however, they do not explicitly map the lane and crosswalk information, which are required for HD maps.

Daniel et. al. [7] fuse semantic images from camera with LiDAR point clouds, but they use real-time raw point clouds from a 64 channel LiDAR, which provides much denser real-time information—while we use a relatively inexpensive 16 channel LiDAR, a trade off between resolution and cost. Additionally, their focus is on off-road terrains, in contrast to our focus: the urban driving scenario. Urban driving scenes require special treatment of the lanes and crosswalks.

Probabilistic Map: Probabilistic maps have been successfully applied to localization [21] [22] and pedestrian motion prediction [23]. Probabilistic maps can capture the inherent distribution information in a discrete space while filtering the noise. In this work, we also demonstrate the successful attempt to apply this techniques to semantic map generation while leveraging the prior information in LiDAR’s intensity channel to produce more stable local maps.

III. METHOD

By fusing a local point cloud map along with semantic images together via geometric transformations, we propose a probabilistic map that can account for the distribution of labels assigned to each grid. As shown in Figure 1, the overall architecture consists of semantic segmentation, point cloud semantic association, semantic mapping, and map transformation.

A. Semantic Segmentation

We use the DeepLabV3Plus [6] network architecture to extract the semantic segmentation from 2D images. Multi-level spatial pyramid CNN layers are used to capture both

the global and local features of the scene. A skip connection is made from the encoder to pass low level image features to the decoder. A lightweight ResNeXt50 [24] pretrained on ImageNet [25] is used as our feature extraction backbone. Compared with other popular backbones like ResNet101 [26], it can achieve the same performance in terms of mean of intersection over union (mIOU) with much fewer parameters and faster inference times. We also adopt the depthwise separable convolution inspired by [6], [27] in our spatial pyramid CNN layers and decoder layers to further improve the inference time while preserving the same performance.

Our semantic segmentation network is trained in Mapillary Vistas dataset [12]. This dataset contains street-level scenes targeted for autonomous vehicle scenarios. It provides a large number of pixel-level semantic segmented images with 66 different kind of labels. We reduce the labels into 19 classes by removing labels that are not essential in our driving environment (e.g. snow) and merging labels with similar semantic meanings together (e.g. zebra line and crosswalk). The rationale behind this step is that we don’t want the network to classify objects that are unlikely to appear in the test environment, or details of which are beyond our interests. The details of label merging can be found in Section IV-A. In the end, there are 19 classes of semantic labels in Mapillary dataset we use to train our network, as presented in Table I. Each label’s associated color is also included in the table.

Training Labels			
curb	crosswalk	road	sidewalk
building	person	bicyclist	motorcyclist
lane marking (white)	sky	vegetation	manhole
pole	traffic-sign	bicycle	bus
car	motorcycle	truck	

TABLE I

TRAINING LABELS AND THEIR ASSOCIATED COLORS FOR THE SEMANTIC SEGMENTATION NETWORK

B. Point Cloud Semantic Association

Given a semantic image, estimating the relative depth for the semantic pixel data can help us reconstruct the 3D scene with semantic labels. This information, however, is usually not available. Depth estimation from multi-view geometry requires salient features, which is prone to error on the road, or when the lighting condition varies a lot. Even with the LiDAR scan that we get at real time, a 16 channel LiDAR's sparse resolution makes it challenging to infer the underlying geometry. Instead our method extracts small regions of a dense point cloud map and projects them into the semantically segmented image to retrieve depth information. Since building such dense point map only requires driving through the area once, this process is less expensive than human labeling.

The transformation from the local point map to the localizer (Velodyne LiDAR) ${}_{vlp}\mathbf{T}_{pm}$ is given by precise centimeter-level localization. We also calibrate the camera with respect to the LiDAR using a non-iterative method solution for the PnP method [28], to estimate their relative transformation: ${}_{cam}\mathbf{T}_{vlp}$. Thus semantic information for a point \mathbf{X}_{pm} can be retrieved from the label of its projected points in image coordinates \mathbf{x}_{img} .

C. Semantic Mapping

While the point cloud with semantic labels provides a 3D reconstruction of the scene, these labels are also subject to noise and small semantic label fluctuations. To address this, a local probabilistic map is constructed and updated using the semantic point cloud.

The local map is a bird eye view in the body frame (rear-axle) of the ego vehicle. We build a local map \mathbf{M}_i at frame i , with the origin defined by pose \mathbf{P}_i , and update it by using the semantic point cloud. Only when the difference of our new pose \mathbf{P}_j and old pose \mathbf{P}_i is beyond a threshold Δ do we construct a new map and transform the old map to it.

Then the projection on the bird's eye view is simply by looking at its x, y component. Discretization by d is applied, and we obtain the corresponding discrete map positions \mathbf{x}_{map} .

We maintain a probabilistic map over a set of semantic labels to capture the latent distribution of semantic points. For each semantic label, we maintain a channel for each cell, representing the relative probability of that label. Originally for each cell, we simply incremented the log odds according to the number of points for each label that project into the cell. However, since the semantic segmentation's quality may degrade at long distances, the map can become overconfident with the wrong labels that it accumulates when the cell is far. To address this problem, a decay process is added when we transform the map.

In addition, we utilize the prior knowledge of correspondences between the LiDAR intensity data and semantic labels to further augment the probabilistic map.

As Figure 2 shows, the zebra lines and side lanes have higher intensity based on the surface reflectivity, suggesting

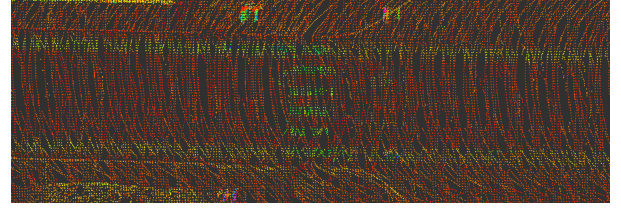


Fig. 2. Intensity of the point cloud

higher chance that this region belongs to specific label. Thus we associate the log-odds with the intensity of that area.

D. Probabilistic Map Transformation

For each frame, we update the probabilistic map with semantic point cloud data, but we do not construct an entirely new local map every frame. Since we only account for a local map and usually our old map and new map have a majority overlap, this transformation can be simplified by a homography, which speeds up the process.

IV. EXPERIMENTS

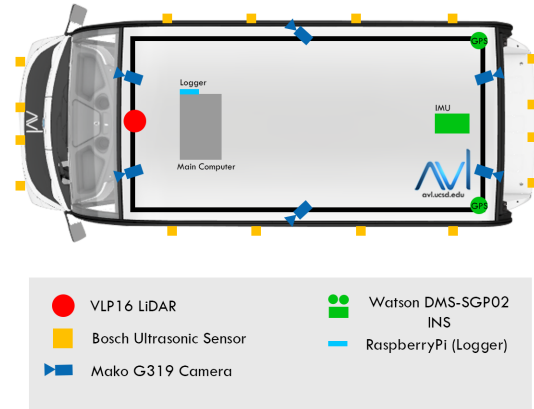


Fig. 3. Vehicle Sensor Configuration

Our experimental data was collected by one of our experimental autonomous cars. The car is equipped with a 16 channel LiDAR and six cameras. The camera's are set up as two on the front, one on each side and two on the back as shown in Figure 3. Data from the front cameras, LiDAR, and vehicle position are recorded for experiments by driving along multiple areas along the UC San Diego campus. The camera data is streamed at around 13 Hz and the LiDAR scan is around 10 Hz. We drive through the campus to collect data for urban driving scenarios—including challenging scenarios like going uphill, downhill, intersections and constructions.

A. Semantic segmentation

Training Dataset: The Mapillary Vistas dataset is split into 18,000 training images and 2,000 validation images. We merge terrain into vegetation, different types of riders into the human category, traffic-sign-back and traffic-sign-front into traffic-sign, bridge into building, and different kinds of

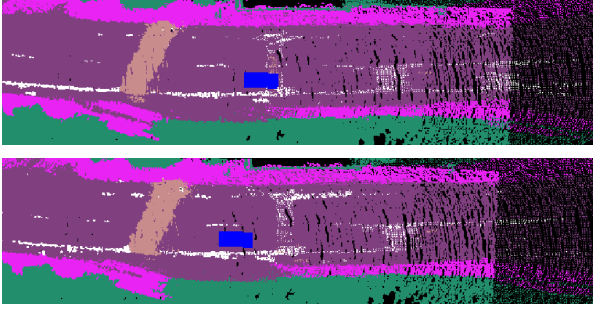


Fig. 4. A comparison between not fusing intensity into semantic mapping (top image) and fusing intensity into probability update (bottom image) achieve slightly better results.

crosswalks into a single crosswalk class. The training dataset is augmented by random horizontal flips with 0.5 probability, random resize with scale ranged from 0.5 to 2, and random crop. These images are also normalized to a distribution with mean of (0.485, 0.456, 0.406) and standard deviation of (0.229, 0.224, 0.225).

Although the network has never been trained on images from UC San Diego campus, we do not observe severe degeneration in our semantic map. The distribution shift across training and testing domains is alleviated due to the similarity of the Mapillary dataset and our driving scenarios, as well as the intense data augmentation in the training process.

Hyperparameters: We use a batch size of 16 with synchronized batch normalization [5] to train our network for 200 epochs on eight 2080Ti GPUs with input image sizes of 640x640. The output stride of the network is 8. We use a SGD optimizer and employ a polynomial learning rate policy [6], [29] where the learning rate is $base_lr \times (1 - \frac{epoch}{max_epoch})^{power}$ with 0.005 base learning rate and power=0.9. The momentum and weight decay are set to 0.9 and $4e^{-5}$, respectively.

Metric: mean intersection over union (mIOU) is used to evaluate the performance of the network. The ResNeXt50 based network achieves 68.32% mIOU whereas the ResNet101 achieves 70.02% mIOU. Although the performance is slightly decreased in the ResNeXt50 network, it has fewer parameters and slightly faster inference times compared to the ResNet101 network. It is thus preferred to be deployed in our autonomous vehicle in which the GPU memory may be more limited. In our cases, the size of the network reduced from 367MB to 210MB (42.78% reduction) and inference time remains at approximately 0.2s.

B. Semantic Mapping

1) *Fuse Intensity:* In Figure 4, we compare the results obtained by incorporating the LiDAR intensity channel to the probabilistic map. Our intuition behind this is that due to poor light conditions, semantic segmentation often fails to capture the true label. After adding the intensity constraint, we achieve slightly better results shown in the bottom figure: the map contains very clear zebra lines and side lanes.

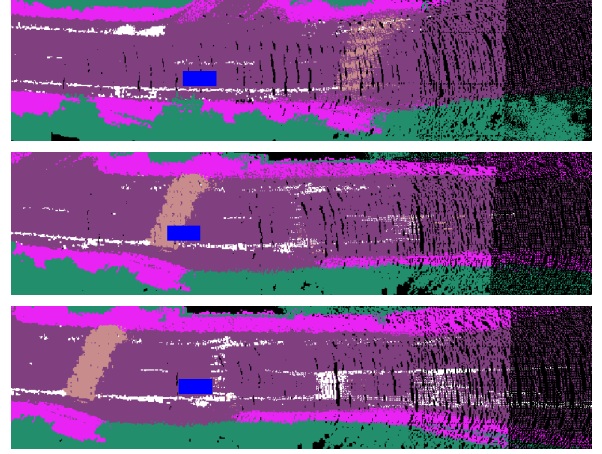


Fig. 5. A sequence of local map shows the automatic correction ability of probabilistic map.

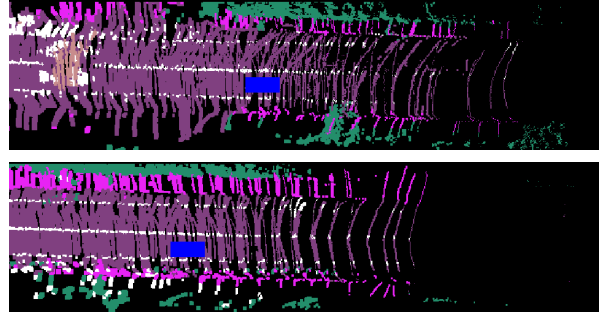


Fig. 6. Semantic mapping using real time LiDAR scan. The bottom image shows that the map become even sparser when the car drive faster.

2) *Probabilistic map fusion:* With the probabilistic modeling approach, the map becomes more and more accurate when more information is available. This can be seen in Figure 5. The crosswalk measurements are initially sparse, but they are corrected as the vehicle drives closer.

C. Comparison to Sparse LiDAR Scan

As previously noted, one possible alternative for extracting the depth information is to use the point cloud data generated by the LiDAR in real time. By following a similar approach, we project the point cloud onto the semantic image frame, and then build the semantic point cloud and semantic local map.

Figure 6 shows that this approach gives relatively accurate point semantic correspondences. This is reasonable since we directly calibrate our camera with respect to the LiDAR. The localization error will not influence the semantic retrieval step. However, for the 16 channel LiDAR that we are using, the scans are too sparse to construct a semantic map in real time since the point cloud resolution increases only when we are close enough. This becomes worse when the car drives faster. Therefore, a prebuilt dense point cloud map allows us to construct semantic maps for longer ranges.

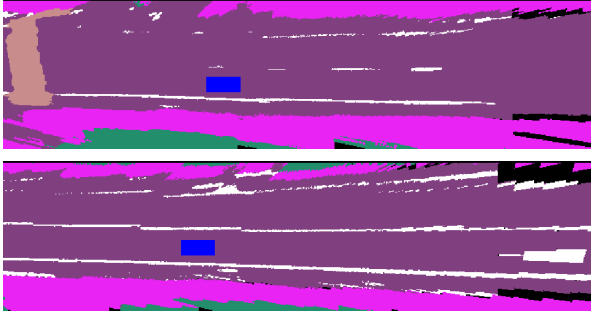


Fig. 7. Using planar assumption to generate dense semantic maps. The reconstructed local map looks smooth when the planar assumption holds, as shown in the top image. However, we can observe surface distortion when this assumption fails, as shown in the bottom image.

D. Comparison to Planar Assumption

Another method explored assumes a flat ground and back projects the semantic images to it. Since this is a plane to plane mapping, a homography \mathbf{H} is calculated in a similar way to the approach that we described to transform the probabilistic map.

The top image in Figure 7 shows that when the ground is flat, the image back projection approach provides dense information. This is because we utilize the 1920×1440 original image, which provides full coverage of the overlap region in the local map. This is two orders of magnitude denser than the dense point map approach, where there are typically at the magnitude of 10K points. However, the planar assumption often fails on road intersections and steep inclines in urban driving scenarios. The bottom image in Figure 7 gives a typical case when the vehicle is going downhill and distortion is observed as a result.

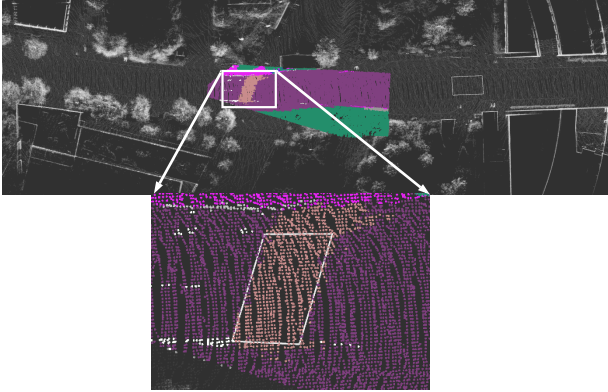


Fig. 8. Comparison with manually labeled HD map: The white box is labeled crosswalk and the pink area corresponds to the semantic point cloud projection.

E. Comparison to HD Map

An HD map was originally created for autonomous mail delivery tasks in the UC San Diego campus [30]. This HD map contains manually annotated road information such as crosswalks, stop lines, sidewalks, and center of road lane

definitions and has been tested in the realistic environments. It is therefore a good testing dataset for evaluating our automatically generated semantic map. Compared with the HD map, our model can help localize crosswalks as shown in Figure 8. A larger map build from the local map is shown in Figure 9 and compared with point cloud map in Figure 10.

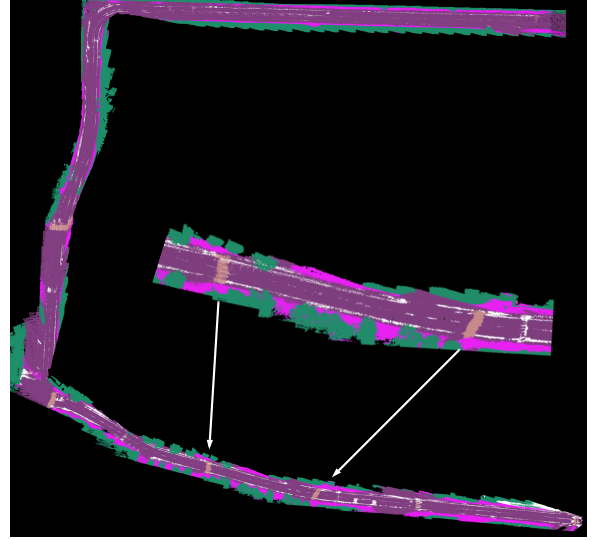


Fig. 9. A larger map composed of multiple local semantic maps, the amplified image highlights the crosswalk localizations.



Fig. 10. The semantic map displayed on top of the point cloud map

V. CONCLUSION

By fusing the rich information from semantic labels on image frames, our comparisons to manually annotated maps indicate that this work effectively introduces a statistical method for identifying road features and localizing them in 3D space that can be applied for automating HD map annotation for crosswalks, lane markings, driveable surfaces and

sidewalks. These features can be incorporated for generating HD maps independently of predefined HD map formats with the additional extension of center lane identifications which are often used for path tracking algorithms.

By accounting for the road network junctions and forks, future work involves the full automation of road network annotations that could leverage graphical methods. While a combination of the techniques proposed can potentially address the scalability drawbacks from HD maps, they also propose new areas of research on high-level dynamic planning. Currently, many autonomous driving architectures require dense point cloud maps for localization and come at a scalability and maintenance cost in a similar way that HD maps do. By dynamically estimating driveable surfaces, traffic lanes, lane markings and other road features, the notion of using centimeter-level localization could be removed as long as immediate actions can be extracted from a high-level planner. In future work, we plan to explore solutions for fully automating the HD mapping process while exploring the idea of dynamic planning without a detailed dense point cloud map.

REFERENCES

- [1] J. Jiao. Machine learning assisted high-definition map creation. In *2018 IEEE 42nd Annual Computer Software and Applications Conference (COMPSAC)*, volume 01, pages 367–373, July 2018.
- [2] B. Douillard, D. Fox, F. Ramos, and H. Durrant-Whyte. Classification and semantic mapping of urban environments. *The International Journal of Robotics Research*, 30(1):5–32, 2011.
- [3] S. Sengupta, P. Sturgess, L. Ladick, and P. H. S. Torr. Automatic dense visual semantic mapping from street-level imagery. In *2012 IEEE/RSJ International Conference on Intelligent Robots and Systems*, pages 857–862, Oct 2012.
- [4] Jonathan Long, Evan Shelhamer, and Trevor Darrell. Fully convolutional networks for semantic segmentation. In *The IEEE Conference on Computer Vision and Pattern Recognition (CVPR)*, June 2015.
- [5] Hengshuang Zhao, Jianping Shi, Xiaojuan Qi, Xiaogang Wang, and Jiaya Jia. Pyramid scene parsing network. *2017 IEEE Conference on Computer Vision and Pattern Recognition (CVPR)*, Jul 2017.
- [6] Liang-Chieh Chen, Yukun Zhu, George Papandreou, Florian Schroff, and Hartwig Adam. Encoder-decoder with atrous separable convolution for semantic image segmentation. *Lecture Notes in Computer Science*, page 833851, 2018.
- [7] Daniel Maturana, Po-Wei Chou, Masashi Uenoyama, and Sebastian Scherer. Real-time semantic mapping for autonomous off-road navigation. In Marco Hutter and Roland Siegwart, editors, *Field and Service Robotics*, pages 335–350, Cham, 2018. Springer International Publishing.
- [8] Gellért Mátyus, Wenjie Luo, and Raquel Urtasun. Deeproadmapper: Extracting road topology from aerial images. In *Proceedings of the IEEE International Conference on Computer Vision*, pages 3438–3446, 2017.
- [9] Namdar Homayounfar, Wei-Chiu Ma, Justin Liang, Xinyu Wu, Jack Fan, and Raquel Urtasun. Dagmapper: Learning to map by discovering lane topology. In *Proceedings of the IEEE International Conference on Computer Vision*, pages 2911–2920, 2019.
- [10] Marius Cordts, Mohamed Omran, Sebastian Ramos, Timo Rehfeld, Markus Enzweiler, Rodrigo Benenson, Uwe Franke, Stefan Roth, and Bernt Schiele. The cityscapes dataset for semantic urban scene understanding. In *The IEEE Conference on Computer Vision and Pattern Recognition (CVPR)*, June 2016.
- [11] Gabriel J. Brostow, Julien Fauqueur, and Roberto Cipolla. Semantic object classes in video: A high-definition ground truth database. *Pattern Recognition Letters*, xx(x):xx–xx, 2008.
- [12] Gerhard Neuhold, Tobias Ollmann, Samuel Rota Bulò, and Peter Kontschieder. The mapillary vistas dataset for semantic understanding of street scenes. In *International Conference on Computer Vision (ICCV)*, 2017.
- [13] Liang-Chieh Chen, George Papandreou, Florian Schroff, and Hartwig Adam. Rethinking atrous convolution for semantic image segmentation, 2017.
- [14] Bichen Wu, Alvin Wan, Xiangyu Yue, and Kurt Keutzer. SqueezeSeg: Convolutional neural nets with recurrent crf for real-time road-object segmentation from 3d lidar point cloud. *2018 IEEE International Conference on Robotics and Automation (ICRA)*, May 2018.
- [15] Robin Heinzler, Florian Piewak, Philipp Schindler, and Wilhelm Stork. Cnn-based lidar point cloud de-noising in adverse weather. *IEEE Robotics and Automation Letters*, 5(2):2514–2521, 2020.
- [16] Yuan Wang, Tianyue Shi, Peng Yun, Lei Tai, and Ming Liu. Pointseg: Real-time semantic segmentation based on 3d lidar point cloud, 2018.
- [17] Lyne Tchapmi, Christopher Choy, Iro Armeni, JunYoung Gwak, and Silvio Savarese. Segcloud: Semantic segmentation of 3d point clouds. *2017 International Conference on 3D Vision (3DV)*, Oct 2017.
- [18] Ioannis Kostavelis and Antonios Gasteratos. Semantic mapping for mobile robotics tasks: A survey. *Robotics and Autonomous Systems*, 66:86 – 103, 2015.
- [19] D. F. Wolf and G. S. Sukhatme. Semantic mapping using mobile robots. *IEEE Transactions on Robotics*, 24(2):245–258, April 2008.
- [20] S. Sengupta, E. Greveson, A. Shahrokni, and P. H. S. Torr. Urban 3d semantic modelling using stereo vision. In *2013 IEEE International Conference on Robotics and Automation*, pages 580–585, May 2013.
- [21] J. Levinson and S. Thrun. Robust vehicle localization in urban environments using probabilistic maps. In *2010 IEEE International Conference on Robotics and Automation*, pages 4372–4378, May 2010.
- [22] Yunming Shao, Charles Toth, Dorota A. Grejner-Brzezinska, and Lowber B. Strange. High-accuracy vehicle localization using a pre-built probability map. 2017.
- [23] J. Wu, J. Ruenz, and M. Althoff. Probabilistic map-based pedestrian motion prediction taking traffic participants into consideration. In *2018 IEEE Intelligent Vehicles Symposium (IV)*, pages 1285–1292, June 2018.
- [24] Saining Xie, Ross Girshick, Piotr Dollar, Zhuowen Tu, and Kaiming He. Aggregated residual transformations for deep neural networks. *2017 IEEE Conference on Computer Vision and Pattern Recognition (CVPR)*, Jul 2017.
- [25] Olga Russakovsky, Jia Deng, Hao Su, Jonathan Krause, Sanjeev Satheesh, Sean Ma, Zhiheng Huang, Andrej Karpathy, Aditya Khosla, Michael Bernstein, Alexander C. Berg, and Li Fei-Fei. ImageNet Large Scale Visual Recognition Challenge. *International Journal of Computer Vision (IJCV)*, 115(3):211–252, 2015.
- [26] Kaiming He, Xiangyu Zhang, Shaoqing Ren, and Jian Sun. Deep residual learning for image recognition. *2016 IEEE Conference on Computer Vision and Pattern Recognition (CVPR)*, Jun 2016.
- [27] Francois Chollet. Xception: Deep learning with depthwise separable convolutions. *2017 IEEE Conference on Computer Vision and Pattern Recognition (CVPR)*, Jul 2017.
- [28] Vincent Lepetit, Francesc Moreno-Noguer, and Pascal Fua. Epanp: An accurate o(n) solution to the pnp problem. *International Journal of Computer Vision*, 81, 02 2009.
- [29] Yi Zhu, Karan Sapra, Fitsum A. Reda, Kevin J. Shih, Shawn Newsam, Andrew Tao, and Bryan Catanzaro. Improving semantic segmentation via video propagation and label relaxation. *2019 IEEE/CVF Conference on Computer Vision and Pattern Recognition (CVPR)*, Jun 2019.
- [30] David Paz, Po-Jung Lai, Sumukha Harish, Hengyuan Zhang, Nathan Chan, Chun Hu, Sumit Binnani, and Henrik Christensen. Lessons learned from deploying autonomous vehicles at UC San Diego. In *Field and Service Robotics*, Tokyo, JP, August 2019.